



Published in final edited form as:

Nat Geosci. 2015 ; 8: 918–921. doi:10.1038/ngeo2574.

LUNAR VOLATILE DEPLETION DUE TO INCOMPLETE ACCRETION WITHIN AN IMPACT-GENERATED DISK

Robin M. Canup¹, Channon Visscher^{1,2}, Julien Salmon¹, Bruce Fegley Jr.³

¹Planetary Sciences Directorate, Southwest Research Institute, Boulder, CO, 80302

²Chemistry and Planetary Sciences, Dordt College, Sioux Center, IA, 51250

³Department of Earth and Planetary Sciences and McDonnell Center for Space Sciences, Washington University, St. Louis, MO, 63130

Abstract

The Moon may have formed from an Earth-orbiting disk of vapor and melt produced by a giant impact.¹ The Moon and Earth's mantles have similar compositions. However, it is unclear why lunar samples are more depleted in volatile elements than terrestrial mantle rocks^{2–3}, given that an evaporative escape mechanism⁴ appears inconsistent with expected disk conditions.⁵ Dynamical models^{6–7} suggest that the Moon initially accreted from the outermost disk, but later acquired up to 60% of its mass from melt originating from the inner disk. Here we combine dynamical, thermal and chemical models to show that volatile depletion in the Moon can be explained by preferential accretion of volatile-rich melt in the inner disk to the Earth, rather than to the growing Moon. Melt in the inner disk is initially hot and volatile-poor, but volatiles condense as the disk cools. In our simulations, the delivery of inner disk melt to the Moon effectively ceases when gravitational interactions cause the Moon's orbit to expand away from the disk, and this termination of lunar accretion occurs prior to condensation of potassium and more volatile elements. Thus, the portion of the Moon derived from the inner disk is expected to be volatile depleted. We suggest that this mechanism may explain part or all of the Moon's volatile depletion, depending on the degree of mixing within the lunar interior.

The Moon and the bulk silicate Earth (BSE) share many compositional similarities, including comparable abundances of refractory elements³ and essentially identical isotopic compositions for many elements.⁸ However it has been known since the return of *Apollo* samples that compared with the BSE, the Moon is more depleted in volatile elements having condensation temperatures < 1100 K in reference solar nebula conditions, including

Correspondences and requests for materials should be directed to R. M. Canup.

Author contributions: RC conceived of the idea, integrated the component models, and wrote the paper. CV performed the chemical modeling and related analysis, JS performed the data analysis for the accretion models, and BF provided the MAGMA model and relevant thermodynamic calculations for K, Na and Zn.

Code and Data Availability

The SyMBA *N*-body accretion code is a freely available extension to the SWIFT package (<https://www.boulder.swri.edu/~hal/swift.html>). Modifications made to SyMBA to model lunar accretion are described in detail in ref. 6. The MAGMA code is distributed upon request (contact B. Fegley), subject to the requirement that publications using it cite the two papers describing the code (refs. 18–19). Data shown in Figures 1–3 is available upon request.

Competing financial interests: The authors declare no competing financial interests.

moderately volatile potassium and sodium, as well as more highly volatile elements, including zinc.²⁻³

The origin of this depletion is poorly understood, and there are no quantitative models of how the Moon's observed pattern of depletion emerged. It appears unlikely to have been inherited from the Moon-forming impactor, because the compositional similarities between the Moon and Earth seem to require a disk with a BSE-like composition.^{1,8} Alternatively volatiles in the protolunar material may have evaporatively escaped.⁹⁻¹¹ Zinc has been cited as evidence of this, because lunar samples show a ~1.1% enrichment in the heavier ⁶⁶Zn isotope compared to terrestrial or Martian samples, suggestive of Rayleigh fractionation during evaporation into a vacuum.^{4,11} However velocities required for escape from the disk exceed those expected for heavy vapor species such as Zn. These might instead escape hydrodynamically if carried by a flow of lighter species,¹⁰ but even the escape of hydrogen may be minimal due to frequent collisions with heavier species.⁵

In the limit of no escape and a closed system, a depletion could instead result if disk volatiles were preferentially accreted by the Earth rather than by the Moon. Taylor et al.² advocated that the lunar depletion pattern is most consistent with incomplete condensation from an initially high temperature vapor, wherein the accretion of condensates by the Moon is "cut off" at a characteristic temperature that allows incorporation of a small component of alkalis (e.g., K and Na) but only a tiny fraction of more volatile elements (e.g., Zn). Neither the mechanism that would produce such a cut off, nor what the relevant cut off temperature would be in an oxygen-rich protolunar disk environment¹², were known. Here we combine dynamical⁶⁻⁷, thermal¹³, and chemical¹² models to show that the disk's evolution naturally provides a cut off at temperatures consistent with the Moon's depletion pattern.

An initial impact-generated disk is likely a two-phase mixture of silicate vapor and melt.^{1,13-15} The disk lies within and beyond the Roche limit, located at about 3 Earth radii.^{1,15} The disk is massive, and so is vulnerable to clumping due to local gravitational instability.^{14,16-17} Exterior to the Roche limit (the "outer disk"), melt clumps are gravitationally stable and mutually accrete into a moon(s).^{6-7,17} Interior to the Roche limit (the "inner disk"), clumps are continually sheared apart by Earth's tidal force, producing a viscosity that causes the disk to spread.^{14,16}

The inner disk is initially hotter than the outer disk, and it cools more slowly due to its smaller surface area and the local production of heat via viscous dissipation.⁵⁻⁶ As a result, the inner disk may be regulated by the two-phase silicate equilibrium for ~ 10² years.^{13-14,17} During this period, the disk's surface density (σ_T), mid-plane temperature (T_c), and gas mass fraction of its atmosphere at the mid-plane (x_c) are related as¹³

$$\sigma_T \approx \left(\frac{\pi}{x_c}\right)^{1/2} \frac{\bar{\mu} P_c H}{RT_c} \left[1 + \left(\frac{C_s T_c}{x_c l} - 2\right) \frac{T_c}{T_0}\right]^{-1/2} \quad (1)$$

where $\bar{\mu} \approx 30 \text{ g mol}^{-1}$ is the effective molecular weight of the vapor, $P_c = P_0 e^{-T_0/T_c}$ is mid-plane pressure (with $P_0 = 3.2 \times 10^{14} \text{ dyne cm}^{-2}$ and $T_0 = 6.0 \times 10^4 \text{ K}$; ref. 14), $H = (2RT_c/\bar{\mu})^{1/2}/\Omega$ (where R is the gas constant and Ω is orbital frequency), $C_s \approx 10^7 \text{ erg g}^{-1} \text{ K}^{-1}$ is the melt's specific heat, and $I = 1.7 \times 10^{11} \text{ erg g}^{-1}$ is the latent heat of vaporization. A gas-poor structure with $x_c \sim \mathcal{O}(10^{-2})$ is possible¹⁴, although recent work^{13,17} argues that a stratified disk with a mid-plane melt layer surrounded by a vapor-rich atmosphere having $\mathcal{O}(10^{-1}) x_c$ is more likely (see Methods).

With time, radiative cooling from the upper and lower surfaces of the disk's atmosphere allows for increased condensation, and σ_T decreases as the disk spreads.¹⁷ Once σ_T falls below $\sim 10^6 \text{ g cm}^{-2}$, the inner disk's silicate vapor may fully condense.^{6,17} Subsequently, T_c likely reflects a balance between viscous dissipation in the mid-plane melt layer, cooling from the surfaces of a volatile-rich atmosphere, and heating of the atmosphere by the Earth's luminosity (see Methods).

Dynamical simulations⁶⁻⁷ predict that the first 40% or more of the Moon's mass accumulates rapidly from material initially in the outer disk (Fig. 1a, "1"). Over a longer, $\approx 10^2 \text{ yr}$ timescale, the inner disk spreads and supplies the remainder of the Moon's mass in the form of clumps that form near the Roche limit (Fig. 1a, "3").⁶ Initially the orbits of such clumps are rapidly driven outward due to resonant interactions with the inner disk, allowing them to be efficiently accreted by the Moon (Fig. 1b).⁶ However as the inner disk dissipates, disk torques weaken, and clumps are instead scattered onto high-eccentricity orbits by the Moon.⁶ Most are then tidally disrupted as their perigees near the Earth's surface before they can accrete onto the Moon. This effect increases with time as the Moon's orbit expands due to both disk torques and repeated scattering events.⁶ The result is a relatively abrupt transition from an accretionary regime – in which the Moon in this case gains 60% of its mass from the inner disk – to a non-accretionary regime – in which clumps originating near the Roche limit contribute little total mass to the Moon (Fig. 1b).

To evaluate the composition of melt clumps formed near the Roche limit, we consider a BSE composition disk and perform thermodynamic equilibrium calculations using the MAGMA code.¹⁸⁻¹⁹ The composition of the melt and co-existing vapor are estimated as a function of T_c for a number of melt and gas species.¹² From this we derive the partial vapor pressure of each species which, in combination with the total bulk elemental inventory of the disk, is used to estimate the relative fraction of each element in the vapor vs. melt phase as a function of T_c and σ_T (see Methods). Clumps that form rapidly via gravitational instability just outside the Roche limit are large ($\gg \text{ km}$) for relevant values of σ_T (e.g., ref. 6), and as such we assume they retain their initial composition as their orbits subsequently evolve.

Fig. 2 shows the predicted degree of vaporization as a function of T_c and σ_T at the Roche limit. The 50% condensation temperatures for Zn, Na and K are given approximately by

$$T_{50}(K) \approx \frac{A}{\log(\sigma_T) - B} \quad (2)$$

where σ_T is in g cm^{-2} , and $(A, B) = (-1.33 \times 10^4, 12.8)$, $(-1.69 \times 10^4, 12.3)$, and $(-1.59 \times 10^4, 11.5)$ are fitting coefficients for Zn, Na, and K, respectively, derived across the ranges $1 < \log(\sigma_T) < 8$ and $1000 < T(K) < 6000$. These condensation temperatures are much higher than reference solar nebula values.²⁰ Equations (1) and (2) imply that for $2 \times 10^7 \sigma_T (\text{g cm}^{-2}) < 10^6$ (corresponding to a uniform surface density inner disk containing between 2.6 and 0.13 lunar masses) and $0.01 < x_c < 1$, the ratio of the mid-plane temperature at the Roche limit to the 50% condensation temperature, (T_c/T_{50}) , will be between 0.98 and 1.2 for K, 1.1 and 1.3 for Na, and 1.5 and 1.8 for Zn, with a relative volatility sequence $K < Na < Zn$. Thus while the inner disk is regulated by the silicate two-phase equilibrium, clumps near the Roche limit will be substantially depleted in K and Na, and extremely depleted in Zn.

Fig. 3a shows the evolution of the inner disk surface density from the Fig. 1 simulation. Fig. 3b compares the estimated mid-plane temperature at the Roche limit for plausible values for x_c to the 50% condensation temperatures from eqn. (2). The predicted clump formation temperature remains near or above T_{50} for K until the Moon has completed $> 98\%$ of its accretion (Fig. 3c) and the efficiency of clump accretion by the Moon has decreased to $\sim 10\%$ (Fig. 1b). The fraction of the Moon's mass derived from the inner disk depends on the initial radial distribution of disk mass,⁶⁻⁷ but in all cases (Supplemental Materials) the cut off in the Moon's accretion of inner disk material occurs at temperatures comparable to or somewhat higher than T_{50} for K. This is consistent both with the observed depletion of K and more volatile elements, and with the lack of depletion of elements substantially less volatile than potassium.

The cut off mechanism we identify causes the portion of the Moon derived from the inner disk to be volatile poor. The volatile content of the portion of the Moon derived from the outer disk is unclear. Rapid escape of an outer silicate two-phase atmosphere might occur,²¹ although perhaps only for overly idealized conditions. In the absence of escape, the first portion of the Moon to form could be volatile-rich, followed by the later accumulation of an overlying 100 to 500 km volatile-poor layer derived from the inner disk. The Moon's observed depletion pattern would then be a function of the degree of mixing between these two reservoirs, which is uncertain.

In the limit of no volatile escape in the outer disk and a well-mixed lunar interior, removal of an element in the final $\sim 60\%$ Moon's mass would result in at most a factor of 2.5 depletion in the bulk Moon relative to the BSE. This is broadly similar to estimated depletions for K and Na, but much smaller than the observed depletion factor of ~ 30 for Zn (Fig. 2b). It is however plausible that internal mixing in the Moon was incomplete. Some evidence suggests that the initial Moon was not fully molten, with a ~ 200 to 1000-km deep magma ocean²² that overlaid a perhaps cooler, sub-solidus interior.²³ The Moon's composition as inferred from samples (i.e., mare basalts) reflects only its upper few hundred kilometers.²⁴ If interior mixing was incomplete, this material would predominantly reflect the depleted, late-added material from the inner disk, with a much larger depletion factor than the well-mixed case. It is also possible that Zn and more volatile elements were further depleted by a secondary process (e.g., later volcanic degassing on the Moon²⁵), implying an initial lunar Zn abundance higher than shown in Fig. 2b.²⁵

Lunar samples exhibit a mass dependent fractionation in Zn compared to the BSE.⁴ In a closed system, equilibrium condensation can enrich the condensate in heavier isotopes compared to the vapor phase, although the degree of fractionation is less than can be achieved through evaporation into a vacuum. Whether the observed isotopic fractionation in Zn can be explained by a closed disk model or would require a subsequent process (e.g., magma ocean outgassing¹¹) is an open issue.

We have modeled an anhydrous disk.¹² The presence of water²⁵ would not change our overall conclusions: it is the silicate two-phase equilibrium that sets the disk's oxygen fugacity and thermal structure as the Moon accretes inner disk material,¹² and Zn(g) will remain the major Zn-bearing gas even in the presence of water vapor. Results here imply that the final portion of the Moon derived from inner disk melt would be very water-poor compared to the disk's total water content, reflecting the limited solubility of H₂O in magmas at relevant disk pressures.^{9,12}

Methods

This paper identifies a novel mechanism capable of explaining part or all of the Moon's volatile depletion pattern, evaluated through what is to our knowledge the first model to consider both the dynamical and thermodynamical evolution of the protolunar material as the Moon accretes after a giant impact. Each of the components of the model is based on current state-of-the-art, but nonetheless still represents an approximated description, as discussed in more detail below. The observed depletions that would result from the proposed mechanism depend primarily on the extent of mixing in the Moon's interior, as discussed above; this is uncertain and merits further consideration.

Dynamical model:

We use results from an accretion model⁶⁻⁷ that considers (*i*) a uniform surface density (σ_T) disk interior to the Roche limit and (*ii*) a condensate outer disk described by an N -body accretion simulation. In reality, σ_T would vary with radius, but T_c varies rather weakly with σ_T (see eqn. 3 below) as the Moon accretes substantial inner disk material. The model⁶⁻⁷ assumes the inner disk maintains a silicate two-phase state until its mass drops below 0.2 lunar masses, comparable to the condition (0.14 lunar masses, see below) obtained with a more realistic treatment¹⁷ with separately evolving melt and vapor phases and radially varying surface densities. Canonical impacts produce primarily condensed outer disks,^{1,15} consistent with (*ii*). However recent alternatives^{15,27-28} produce highly vaporized disks. In these cases, outer disk vapor might condense over \sim a decade in the absence of local viscous heating, and this timescale could still be shorter than the inner disk lifetime ($\sim 10^2$ yr), leading to a similar overall evolution. However the initial evolution of a highly vaporized disk remains uncertain and different evolutions are conceivable.²¹

We consider that in the inner disk, tidal disruption of clumps produces a viscosity¹⁶ $\nu \approx \pi^2 G^2 \sigma_m^2 / \Omega^3$, where σ_m is the melt surface density, $\Omega = \sqrt{GM_\oplus / r^3}$ is orbital frequency, G is the gravitational constant, M_\oplus is the Earth's mass, and r is orbital radius. The Moon's accretion may be characterized by 3 stages.⁶ Condensed material outside the Roche limit

rapid accretes into a moonlet(s) (“phase 1” in Fig. 1a). Moonlets that accrete in the outer disk interact with the inner disk through resonant torques, which cause their orbits to expand while opposing the outward viscous diffusion of the inner disk.^{6–7,17} A nearby moonlet becomes able to confine the inner disk’s outer edge to within the Roche limit once the moonlet’s mass exceeds $\mathcal{O}(10^{-1})$ lunar masses^{6–7,17}, which initially shuts off its accretion of inner disk material (“phase 2” in Fig. 1a). As the moonlet’s orbit expands, its resonances leave the disk and the inner disk is freed to spread. As inner disk melt spreads beyond the Roche limit, it forms large clumps through local gravitational instability that can be accreted by the growing moon(s) or scattered back into the inner disk or onto the Earth (“phase 3” in Fig. 1a).^{6–7}

The volatile depletion mechanism identified here occurs during phase 3, when the Moon acquires up to about half of its mass from clumps formed at the Roche limit. Such a phase will occur so long as once the Moon’s accumulation commences, the timescale for accretion of material outside the Roche limit is short compared to the lifetime of the inner disk. This appears a good assumption for disks produced by canonical impacts,^{1,15} and perhaps for disks produced by high angular momentum impacts,^{15,27–28} although the latter might evolve substantially prior to the commencement of accretion. Our model assumes that during this final phase of the Moon’s growth, the dominant source of viscosity in the inner disk is associated with the melt, so that melt is driven radially outward while inner disk vapor stays largely in place until it condenses.^{17,29} It is however possible that the vapor could be viscous, and vapor that spread outward during phase 3 and subsequently condensed in the cooler outer disk could (depending on the radial distance traveled prior to condensation) add volatile-rich material to the Moon that is not accounted for in our model. Viscosity in a gas disk is often parameterized as $\nu_{gas} = \alpha_g c^2 / \Omega$, where α_g is a dimensionless parameter and c is the sound speed. Laboratory estimates suggest that hydrodynamic turbulence due to Keplerian shear produces^{30–31} $\alpha_g < 10^{-5}$; such a low α_g would imply a vapor mass flux across the Roche limit substantially smaller than the flux of melt due to the instability-induced viscosity considered here. Efficient diffusive mixing between the disk’s vapor and the Earth’s silicate vapor atmosphere has been proposed as a means to equilibrate Earth-Moon isotopic compositions;³² this mechanism requires the mixing be accompanied by minimal angular momentum transport,³³ also implying a small effective α_g . A large vapor viscosity, with $\alpha_g \sim \mathcal{O}(10^{-2})$, would be associated with active magneto-rotational instability (MRI), but this could be difficult to achieve in a two-phase protolunar disk where orbital frequencies are high and ongoing condensation/settling of silicates (as well as more refractory grains) would tend to reduce the disk ionization fraction.³⁴

Thermal model:

We assume an initial inner disk that is regulated by the silicate two-phase equilibrium,^{13,14,17} with a photospheric temperature $T_{ph} \sim 2000$ K and T_c given by eqn. (1) for a given (σ_T, x_c) . The time evolution of σ_T is provided by the accretion model. We consider a range of plausible x_c values motivated by protolunar disk models.^{13,14,17,29} After the giant impact, the inner disk may rapidly adjust to a state in which there is local vertical thermal balance between viscous dissipation, release of latent heat due to condensation, and radiative cooling from the photosphere.^{13,14,17} In a two-phase silicate disk, this can be accomplished through

either^{13,17} *i*) a vertically well-mixed disk with a very low gas mass fraction, in which the two-phase sound speed is regulated to the point of marginal instability (implying $x_c \sim \alpha(10^{-2})$, refs. [13-14]), or *ii*) a vertically stratified disk, in which the surface density of a gravitationally unstable mid-plane melt layer adjusts itself through condensation or evaporation until thermal balance is achieved [13,17]. Case (*ii*) implies a total magma layer mass of about 0.14 lunar masses, with the remainder of the inner disk mass contained in an overlying vapor-rich atmosphere with $\alpha(10^{-1}) x_c = 1$ (refs. 13,17). Case (*ii*) may be more likely, due to rapid settling of melt droplets to the mid-plane.^{13,17,29} The assumption of two-phase equilibrium implies an intimate mixture of gas and liquid including in the mid-plane, i.e., $x_c > 0$. This is probable in the region interior to the Roche limit, because gravitational stirring by temporary instability-induced clumps will maintain a finite melt layer thickness and a corresponding spatial density of melt much less than the density of a continuous fluid,^{16,29} implying dispersed clumps and droplets with intervening vapor-filled space.

We consider that instability-induced clumps will form near the disk mid-plane at temperature T_c . Silicate droplets will condense at altitude, but settle rapidly while still small.²⁹ For relevant values of σ_T (between 10^6 and $\text{few} \times 10^7 \text{ g cm}^{-2}$), we find that T_c from eqn. (1) is well approximated by (see Fig. 4s in supplemental materials)

$$T_c \approx T_1 \left(\frac{\sigma_T}{10^7 \text{ g cm}^{-2}} \right)^\alpha \quad (3)$$

where T_1 and α are fitting factors, with $T_1 = 3560 \text{ K}$ and $\alpha = 0.063$ for $x_c = 0.01$, $T_1 = 3740 \text{ K}$ and $\alpha = 0.065$ for $x_c = 0.1$, and $T_1 = 4010 \text{ K}$ and $\alpha = 0.07$ for $x_c = 1$. The appropriate value for x_c near the Roche limit may evolve with time. Thus the mid-plane temperature evolution would be expected to lie between the $x_c = 0.01$ and $x_c = 1$ curves in Fig. 3b. Eqns. (1) and (3) ignore heating by the Earth. After the giant impact, Earth's atmosphere may rapidly adjust to a radiating temperature¹⁴ $T_\oplus \sim 2000$ to 2500 K . Because the planet's luminosity decreases as approximately $(1/r)^2$ and $T_\oplus \sim T_{ph}$ while the disk is in a two-phase silicate state, Earth shine is a minor influence on the disk's temperature near the Roche limit during this phase.

We assume the inner disk's silicate vapor fully condenses once $\sigma_T < 1.7 \times 10^6 \text{ g cm}^{-2}$, as in ref (6). Subsequently we estimate T_{ph} assuming a balance between viscous dissipation in the mid-plane (with rate per area $\dot{E}_v = 9 \sigma_m \nu \Omega^2 / 4$, Earth shine on the upper and lower surfaces of the disk's volatile-rich atmosphere (with rate per area \dot{E}_\oplus , and radiative cooling from these surfaces, with

$$2 \sigma_{SB} T_{ph}^4 = \dot{E}_\oplus + \dot{E}_v \quad (4)$$

$$\approx 2 \sigma_{SB} T_{\oplus}^4 \left[\frac{2}{3\pi} \left(\frac{R_{\oplus}}{r} \right)^3 + \frac{1}{2} \left(\frac{R_{\oplus}}{r} \right)^2 \left(\frac{3-\beta}{2} - 1 \right) \left(\frac{c}{r\Omega} \right) \right] + \frac{9\pi^2 G^2 \sigma_m^3}{4\Omega},$$

where σ_{SB} is the Stefan-Boltzmann constant, $T_c(r) \propto (1/r)^\beta$, implying an atmosphere scale height that increases with radius as $H \propto r^{3/2 - (\beta/2)}$ and the expression for \dot{E}_{\oplus} is from ref. [35], eqn. B4. A corresponding estimate for T_c is³⁶

$$2 \sigma_{SB} T_c^4 \approx \left(1 + \frac{3}{8} \kappa \sigma_v \right) \dot{E}_v + \dot{E}_{\oplus}. \quad (5)$$

For $\sigma_T \sim 10^6 \text{ g cm}^{-2}$ (i.e., the later evolution in Fig. 3) and an anhydrous BSE composition disk¹², expected vapor surface densities are $\sigma_v \sim 10^4 \text{ g cm}^{-2}$ to 10^2 g cm^{-2} as the disk cools from $\sim 3000 \text{ K}$ to $\sim 1800 \text{ K}$ (see Supplemental Material Fig. 5S). An additional 1000 ppm H₂O would provide up to $\sigma_v \sim 10^{-3} \sigma_T \text{ g cm}^{-2}$ across this temperature range,¹² or $\sigma_v \sim 10^3 \text{ g cm}^{-2}$ for $\sigma_T \sim 10^6 \text{ g cm}^{-2}$. Either implies $\sigma_v \ll \sigma_m \approx \sigma_T$ in the disk's later phase. The atmospheric opacity κ is uncertain, with $\kappa \sim 10^{-2} \text{ cm}^2 \text{ g}^{-1}$ estimated for relevant densities and temperatures for a solar composition gas.³⁷ In Fig. 3b, we simply set $(\kappa \sigma_v) = 10$. In the case of a much higher opacity (such as would apply if silicate droplets contribute significantly), the implied temperature gradient from (5) would be super-adiabatic, and in this case the vertical heat flux would likely be convectively rather than radiatively transported, resulting in an adiabatic temperature gradient.¹³ Our conclusions are not sensitive to the treatment of T_c in this phase since by this time the Moon has essentially completed its accretion.

Chemical Model:

The MAGMA code¹² is used to calculate for a given T_c the partial pressure of each gas species i (P_i) in equilibrium with the multicomponent silicate melt, with $P_i = x_i P_T$ where x_i is the mole fraction abundance of each gas and P_T is the total pressure. We relate the partial pressure of each species to its vapor surface density ($\sigma_{i,v}$) as $P_i = \rho_i RT_c / \mu_i \approx \sigma_{i,v} RT_c / (2H\mu_i)$, where ρ_i and μ_i are the vapor density and molecular weight of species i , and $H \approx \sqrt{2}c/\Omega$ is the disk's scale height, with sound speed $c = \sqrt{\bar{\gamma} RT_c / \bar{\mu}}$, mean atmospheric adiabatic index $\bar{\gamma}$ and molecular weight $\bar{\mu}$, and Ωc calculated at the Roche limit. The vapor surface density of each gas species and the total vapor surface density are

$$\sigma_{i,v} \approx \frac{2P_i \mu_i}{\Omega} \sqrt{\frac{2\bar{\gamma}}{RT_c \bar{\mu}}}; \quad \sigma_v \approx \frac{2P_T}{\Omega} \sqrt{\frac{2\bar{\gamma} \bar{\mu}}{RT_c}} \quad (6)$$

where $\sigma_v = \sum_i \sigma_{i,v}$ given $P_T = \sum_i P_i$.

The total vapor density for each element is determined by adding the contributions of each gas species i containing element M ,

$$\sigma_{M,v} = \sum_i \frac{n_{M(i)} \mu_M}{\mu_i} \sigma_{i,v}, \quad (7)$$

where μ_M is the atomic weight of element M and $n_{M(i)}$ is the stoichiometric coefficient for element M in species i ($n_{Si(SiO_2)} = 1$, $n_{O(SiO_2)} = 2$, etc.). Once element vapor densities are known, the relative fraction of each element in vapor versus melt can be determined for a given total surface density of melt and vapor. The bulk inventory of each element is given by $\sigma_M = w_M \sigma_T$, where σ_M is the total surface density (melt + vapor) of element M , w_M is the mass fraction of element M in the system, and σ_T is the total surface density of the melt and vapor disk ($\sigma_T = \sigma_M + \sigma_v$). The mass fraction of each element that is vaporized is $m_{vap} = \sigma_{M,v} / \sigma_M$.

MAGMA assumes a melt phase is always present, i.e., that there is in effect an inexhaustible supply of BSE composition material. Without modification, this would lead to unrealistically large estimates for σ_v and P_T for the situation considered here, in which there is a finite local supply of melt. As such we impose the additional requirement that $\sigma_{M,v} \leq \sigma_M$, i.e., that the vapor surface density for each element (and therefore its partial pressure per eqns. 5 and 6) has a maximum value set by the element's total (bulk) inventory in the disk. This can be seen in Figures 2 and 5s, where the estimated vapor density of each element increases with temperature until $\sigma_{M,v} \approx \sigma_M$, whereupon the density remains constant. We approximate T_{50} as the temperature at which $\sigma_{M,v} = 0.5 \sigma_M = 0.5 w_M \sigma_T$, so that T_{50} is ultimately a function of melt-vapor equilibria (and therefore T_c), the bulk element inventory (assumed here to correspond to a BSE composition), and the disk surface density. Resulting condensation temperatures are approximations, but should provide reasonable estimates for the expected behavior. Our predicted T_{50} values for Na and K are broadly similar to those recently reported for Na and K using a different approach³⁸, particularly for the regime of interest as the Moon accretes inner disk material ($\sigma_T > 10^6 \text{ g cm}^{-2}$ and approximately $>$ a few bar pressure).

Supplementary Material

Refer to Web version on PubMed Central for supplementary material.

Acknowledgements:

We thank D. Stevenson for comments and suggestions. Funding from NASA's Solar System Exploration Research Virtual Institute (*SSERVI*, for RC, CV and JS), NASA's Lunar Advanced Science and Exploration Research program (*LASER*, for RC), and from NSF's Planetary Astronomy program (grant 1412175, for BF) is gratefully acknowledged.

References

1. Canup RM Lunar-forming impacts: Processes and alternatives. *Philosophical Transactions of the Royal Society A* 372, 20130175 (2014).
2. Taylor SR, Taylor GJ & Taylor LA, The Moon: A Taylor perspective. *Geochimica et Cosmochimica Acta* 70 (24), 5904–5918 (2006).
3. Taylor GJ & Wieczorek MA Lunar bulk chemical composition: A post-Gravity Recovery and Interior Laboratory reassessment. *Philosophical Transactions of the Royal Society A* 372, 20130242 (2014).
4. Paniello RC, Day JMD & Moynier F, Zinc isotopic evidence for the origin of the Moon. *Nature* 490 (7420), 376–379 (2012). [PubMed: 23075987]
5. Nakajima M & Stevenson DJ Hydrodynamic escape does not prevent the “Wet” Moon formation. 45th Lunar and Planetary Science Conference 2770 (2014).
6. Salmon J & Canup RM, Lunar Accretion from a Roche-interior Fluid Disk. *The Astrophysical Journal* 760 (1) (2012).
7. Salmon J & Canup RM, Accretion of the Moon from non-canonical discs. *Philosophical Transactions of the Royal Society A* 372, 20130256 (2014).
8. Dauphas N, Burkhardt C, Warren PH & Teng F-Z Geochemical arguments for an Earth-like Moon-forming impactor. *Philosophical Transactions of the Royal Society A* 372, 20130244 (2014).
9. Desch SJ & Taylor GJ, A Model of the Moon’s Volatile Depletion, 42nd Lunar and Planetary Science Conference, 2005 (2011)
10. Desch SJ & Taylor GJ, Isotopic Mixing due to Interaction Between the Protolunar Disk and the Earth’s Atmosphere, 44th Lunar and Planetary Science Conference, 2566 (2013).
11. Day JMD & Moynier F, Evaporative fractionation of volatile stable isotopes and their bearing on the origin of the Moon. *Philosophical Transactions of the Royal Society A* 372, 20130259 (2014).
12. Visscher C & Fegley B Jr., Chemistry of Impact-generated Silicate Melt-vapor Debris Disks. *The Astrophysical Journal Letters* 767 (1), L12 (2013).
13. Ward WR, On the Vertical Structure of the Protolunar Disk. *Astrophysical Journal* 744 (2), 140 (2012).
14. Thompson C & Stevenson DJ, Gravitational instability in two-phase disks and the origin of the moon. *Astrophysical Journal* 333, 452–481 (1988).
15. Nakajima M & Stevenson DJ, Investigation of the initial state of the Moon-forming disk: Bridging SPH simulations and hydrostatic models. *Icarus* 223, 259–267 (2014).
16. Ward WR & Cameron AGW, Disc Evolution Within the Roche Limit, 9th Lunar and Planetary Science Conference, 1205–1207 (1978).
17. Ward WR, On the evolution of the protolunar disc. *Philosophical Transactions of the Royal Society A* 372, 20130250 (2014).
18. Fegley B Jr. & Cameron AGW, A vaporization model for iron/silicate fractionation in the Mercury protoplanet. *Earth and Planetary Science Letters* 82, 207–222 (1987).
19. Schaefer L & Fegley B Jr. A thermodynamic model of high temperature lava vaporization on Io. *Icarus* 169 (1), 216–241 (2004).
20. Lodders K Solar system abundances and condensation temperatures of the elements. *Astrophysical Journal* 591, 1220–1247 (2003).
21. Genda H & Abe Y Modification of a proto-lunar disk by hydrodynamic escape of silicate vapor. *Earth Planets Space* 55, 53–57 (2003).
22. Elkins-Tanton LT, Burgess S, & Yin Q-Z The lunar magma ocean: Reconciling the solidification process with lunar petrology and geochronology. *Earth and Planetary Science Letters* 304, 326–336 (2011).
23. Andrews-Hanna JC et al., Ancient igneous intrusions and early expansion of the Moon revealed by GRAIL gravity gradiometry. *Science* 339 (6120), 675–678 (2013). [PubMed: 23223393]
24. Longhi J Experimental petrology and petrogenesis of mare volcanics. *Geochimica et Cosmochimica Acta* 56, 2235–2251 (1992).

25. Hauri EH, Saal AE, Rutherford MJ, & Van Orman JA Water in the Moon's interior: Truth and consequences. *Earth and Planetary Science Letters* 409, 252–264 (2015).
26. Albarede F, Albalat E, & Lee C-T A. An intrinsic volatility scale relevant to the Earth and Moon and the status of water in the Moon. *Meteor. & Planet. Sci.* 50, 568–577 (2015).

Method References

27. Cuk M & Stewart ST, Making the Moon from a Fast-Spinning Earth: A Giant Impact Followed by Resonant Despinning. *Science* 338, 1047–1052 (2012). [PubMed: 23076099]
28. Canup RM, Forming a Moon with an Earth-like Composition via a Giant Impact. *Science* 338, 1052–1055 (2012). [PubMed: 23076098]
29. Machida R & Abe Y The evolution of an impact-generated partially vaporized circumplanetary disk. *Astrophys J.* 617:633–644 (2004).
30. Ji H, Burin M, Scharfman E & Goodman J Hydrodynamic turbulence cannot transport angular momentum effectively in astrophysical disks. *Nature* 444, 343–346 (2006). [PubMed: 17108959]
31. Edlund EM & Ji H Nonlinear stability of laboratory quasi-Keplerian flows. *Phys. Rev. E*, 89, 021004 (2014).
32. Pahlevan K & Stevenson DJ Equilibration in the aftermath of the lunar-forming giant impact. *Earth Planet. Sci. Lett.* 262, 438–449 (2007).
33. Melosh HJ New approaches to the Moon's isotopic crisis. *Philosoph. Trans. Roy. Soc. A.* 372: 20130168, 1–12 (2014).
34. Fujii YI, Ozuzumi S, Tanigawa T, & Inutsuka S On the viability of the magnetorotational instability in circumplanetary disks. *Astrophys. J.* 785: 101, 1–8, (2014).
35. Ruden SP & Pollack JB, The dynamical evolution of the protosolar nebula. *Astrophys J.* 375, 740–760 (1991).
36. Nakamoto T & Nakagawa Y Formation, early evolution, and gravitational stability of protoplanetary disks. *Astrophys. J.* 421, 640–650 (1994).
37. Marigo P & Aringer B Low-temperature gas opacity. *Astronomy & Astrophysics* 508, 1539–1569 (2009).
38. Petaev MI, Jacobsen SB, & Huang S Testing models of the Moon's origin, II: Phase relation in a proto-lunar disk of the BSE composition. 46th Lunar and Planetary Science Conference, 2245 (2015).

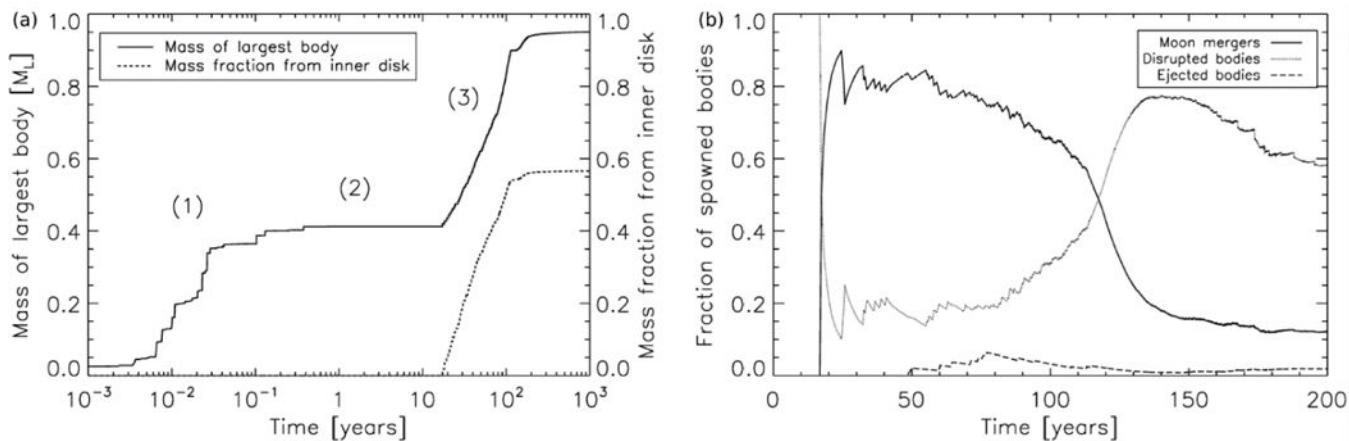


Figure 1–. Simulation of the Moon’s accretion, reproduced from ref. 6. (a) Moon mass vs. time. Outer disk material rapidly accretes into a moonlet containing ~40% of the Moon’s mass (1), and then accretion stalls (2). After ~ 20 yr, inner disk melt spreads beyond the Roche limit and supplies the final 60% of the Moon’s mass (3). (b) Fate of inner disk clumps vs. time. Initially clumps spawned near the Roche limit efficiently merge with the Moon, but a cut off occurs at ~ 120 yr. Subsequently most are scattered toward the Earth, tidally disrupted, and ultimately accreted by the Earth.

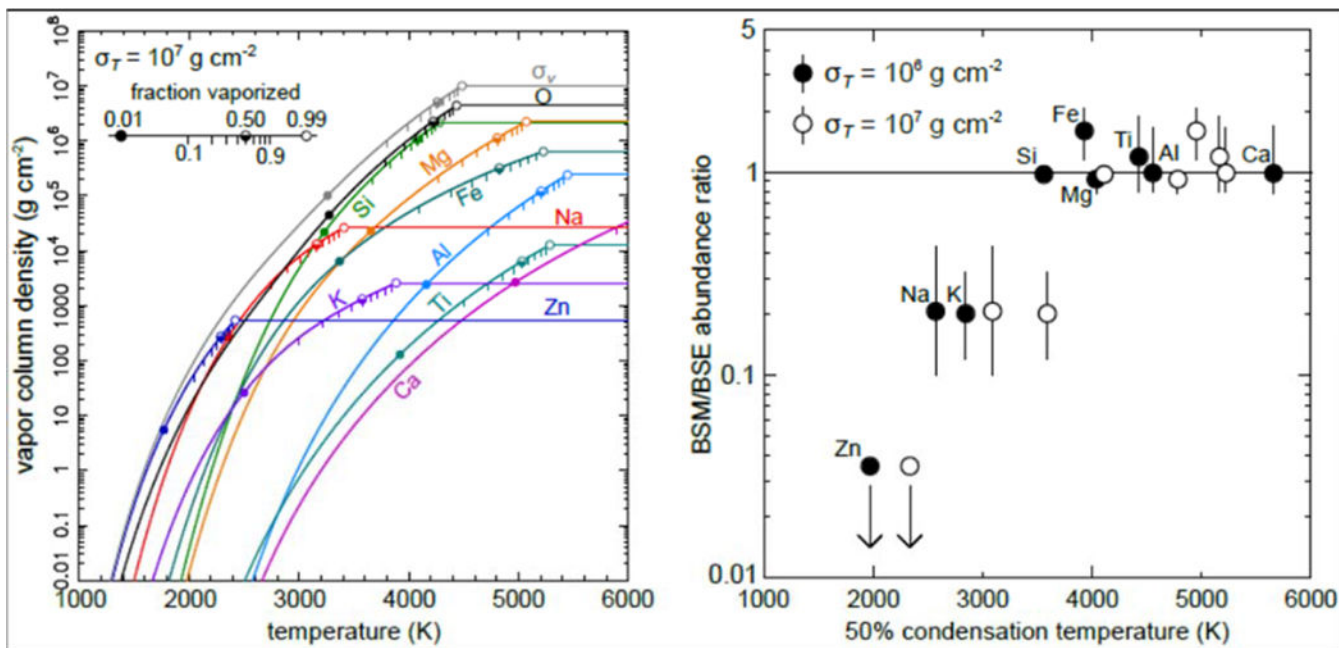


Figure 2. Melt-vapor equilibria in a BSE-composition protolunar disk. (left) Vapor surface density (g cm^{-2}) of each element and the total vapor surface density (σ_v) as a function of temperature at the Roche limit for $\sigma_T = 10^7 \text{ g cm}^{-2}$. Vertical marks indicate mass fraction in the vapor phase from 0.1 to 0.9; symbols indicate 1% (\bullet), 50% (\ominus) and 99% (\circ) vaporization. (right) Observed bulk silicate Moon, BSM, scaled to BSE abundances (with values from ref. 12 and references therein), versus T_{50} values for $\sigma_T = 10^6$ and 10^7 g cm^{-2} estimated here. Arrows for Zn reflect more recent estimates.^{3,26}

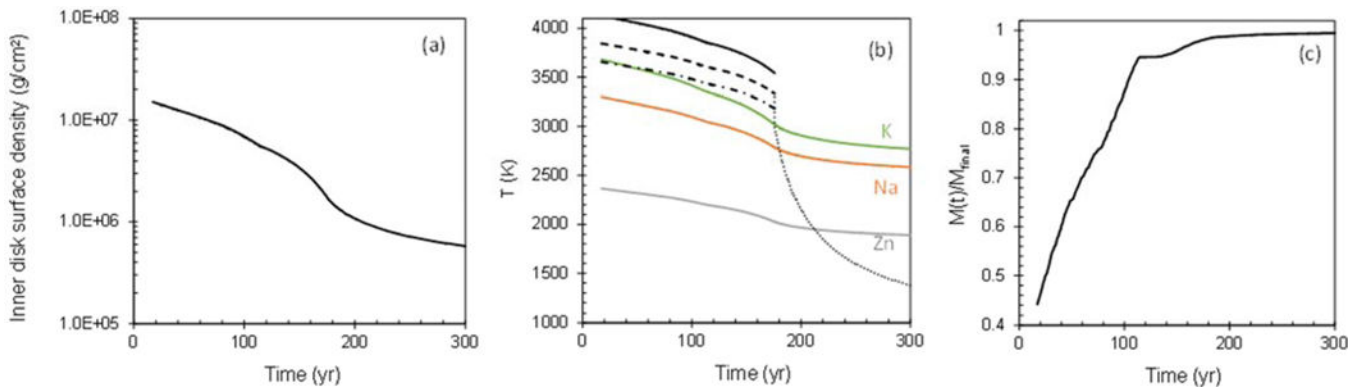


Figure 3—.

Clump formation temperature and volatile content. (a) Inner disk surface density (σ_T) vs. time from the Fig. 1 simulation. (b) Mid-plane temperature at the Roche limit vs. time. Solid, dashed, and dot-dashed lines use eqn. (1) with $x_c = 1, 0.1,$ and $0.01,$ respectively, and $\sigma_T(t)$ from (a). Dotted curve assumes $\kappa\sigma_v = 10,$ $T_\oplus = 2300\text{ K}, \beta = 0.3,$ and $c/r\Omega = 0.2$ (see Methods). Green, orange, and grey curves show estimated T_{50} values (eqn. 2). (c) The Moon's mass scaled to its final mass (M_{final}) from the Fig. 1 simulation. The Moon accretes only ~ a percent of its mass after T_c falls substantially below T_{50} for potassium.